Hindawi Publishing Corporation
Journal of Nanomaterials
Volume 2012, Article ID 720491, 12 pages
doi:10.1155/2012/720491

Research Article

Enhanced Visible-Light Photocatalytic Performance of Nanosized Anatase TiO_2 Doped with CdS Quantum Dots for Cancer-Cell Treatment

Kangqiang Huang,[1] Li Chen,[2] Jieguan Deng,[3] and Jianwen Xiong[1]

[1] *Laboratory of Quantum Information Technology, School of Physics and Telecommunication Engineering, South China Normal University, Guangzhou 510006, China*
[2] *School of Physics and Optoelectronic Engineering, Guangdong University of Technology, Guangzhou 510006, China*
[3] *Institute of Physics, Lanzhou University, Lanzhou 730107, China*

Correspondence should be addressed to Jianwen Xiong, jwxiong@scnu.edu.cn

Received 26 April 2012; Accepted 22 June 2012

Academic Editor: Jiaguo Yu

CdS quantum-dots-(QDs-)doped TiO_2 nanocomposites were successfully synthesized using the sol-gel technique and characterized by SEM, TEM, XRD, EDS, UV-Vis, and FS. They were then used as a new "photosensitizer" based on photodynamic therapy (PDT) for cancer-cell treatment. The photocatalytic activities of CdS-TiO_2 on leukemia tumors were investigated by using Cell Counting Kit-8 (CCK-8) assay. The ultrastructural morphology of treated cells was also studied by AFM. The experimental results indicated that an obvious inhibition of tumor growth would be observed in groups treated with CdS-TiO_2 nanocomposites, and the PDT efficiency in the presence of CdS-doped TiO_2 was significantly higher than that of TiO_2, revealing that the photocatalytic activities of TiO_2 could be effectively enhanced by the modification of CdS QDs. Additionally, CdS- TiO_2 can exhibit a very high photodynamic efficiency of 80.5% at a final concentration of 200 μg/mL under visible-light irradiation. CdS-TiO_2 nanocomposites in this case were regarded as a promising application for cancer-cell treatment.

1. Introduction

Titanium dioxide (TiO_2) as the most promising photocatalyst has been widely used for industrial and medical applications owing to its various advantages (including nontoxicity, low cost, high activity, and strong stability) in the last two decades [1–5]. Under UV radiation, photoinduced electrons and holes could be generated on the TiO_2 surface; these excited electrons and holes have strong reduction and oxidation power, respectively, and could further react with hydroxyl ions or water, resulting in the formation of various reactive oxygen species (ROS) [6–8].

In recent years, research involving use of TiO_2 in biomedical fields has also attracted much attention; TiO_2 nanoparticles for phototherapy of cancer cells and bacteria have been noticed [9–12]. Therefore, TiO_2 nanoparticles are in this case regarded as one of the promising photosensitizers against cancer for photodynamic therapy (PDT). However, the practical application of TiO_2 has been restricted due to its wide band gap (3.2 eV for anatase phase) and low quantum efficiency which greatly reduce the photocatalytic activities of TiO_2 [13, 14]. Fortunately, many previous studies have shown that the photocatalytic activity of TiO_2 can be effectively improved by the method of metal or nonmetal elements doping [15–18]. Meanwhile, it is now well demonstrated that the photocatalytic activities of TiO_2 nanoparticles depend not only on the properties of the TiO_2 material itself, but also on the performance of the modified material [19–21]. Compared with other dopants, semiconductor quantum dots (QDs) have attracted considerable interest in bioengineering and biomedical fields because of their unique optical and electrical properties [22–25]. Additionally, little detailed study has been devoted to CdS-TiO_2 nanocomposites-based PDT for cancer treatment.

Therefore, we aim to modify TiO_2 with a narrow bandgap semiconductor (CdS) to realize visible-light absorbance and improve the charge separation efficiency thus enhancing its photocatalytic activity.

In the present work, CdS-doped TiO_2 nanocomposites were used as a photosensitizer-based PDT for cancer treatment in vitro. To our knowledge, this is the first report to demonstrate the photokilling effect of CdS-TiO_2 nanocomposites on leukemia HL60 cells under visible light irradiation. The aims of the present study were focused on the potential therapeutic effect of CdS-TiO_2 nanocomposites.

2. Materials and Methods

2.1. Chemicals and Apparatus. HL60 cells were kindly provided by the Department of Medicine of Sun Yat-sen University. Cell Counting Kit-8 (CCK-8) assays were purchased from Dojindo (Japan). RPMI medium 1640 and Fluo-3 AM were obtained from Gibco BRL and Sigma (USA), respectively. $Ti(OBu)_4$, mercaptopropionic acid (MPA), $CdC1_2$, and Na_2S were obtained from Soju Blo Co., Ltd. (China). All chemicals used were of analytical reagent or the best commercially available grade. The stock solutions of the compounds were prepared in double-distilled water immediately before using in experiments.

These apparatuses, including ZEISS Ultra-55 scanning electron microscope (Carl Zeiss, Germany), JEM-2100HR transmission electron microscope (JEOL, Japan), Energy Dispersive Spectrometer (Carl Zeiss, Germany), Atomic force microscopy (Bruker, USA), U-3010 UV-visible spectrophotometer (Hitachi, Japan), F-4500 Fluorescence spectrophotometer (Hitachi, Japan), The Countess Automated Cell Counter (Invitrogen, USA), A photodiode (Hitachi, Japan), Model 680 Microplate Reader (Bio-Rad, USA), HH.CP-TW80 CO_2 incubator, and PDT reaction chamber, and so on were used in this research.

2.2. Preparation of CdS QDs-Doped TiO_2 Nanocomposites

2.2.1. Preparation of CdS QDs Solutions. The CdS precursor solution was prepared by adding freshly 10 mL of Na_2S solution to 100 mL of prepared $CdC1_2$ solution in the presence of mercaptopropionic acid (MPA) as the stabilizer under vigorous stirring ($[CdC1_2] = 1.0 \times 10$ mol/L, [MPA] $= 2.0 \times 10$ mol/L, and $[Na_2S] = 1.0 \times 10$ mol/L). Meanwhile, the solution pH was adjusted to 3.0 by HCl at a concentration of 0.01 mol/L. Afterwards the mixture solution was heated to 80°C. Since a longer heating time resulted in a larger particle size, the desired size of CdS was determined by controlling the heating time [26]. Finally, the formed CdS colloid was dialyzed exhaustively against water overnight at room temperature to obtain CdS(QDs) solution.

2.2.2. Synthesis of CdS-TiO_2 Nanocomposites. The CdS-TiO_2 nanocomposites were synthesized by a sol-gel method similar to that described by Wang et al. [27, 28], but with minor modifications. Briefly, $Ti(OBu)_4$, which was chosen as a Ti precursor, was dissolved in 20.0 mL ethanol in the presence of iminodiacetic acid (the solution pH was adjusted to 7.0). After $Ti(OBu)_4$ was hydrolyzed completely, the resulting solution was kept stirring for 2 hours under mild conditions. Subsequently, a definite volume of the prepared CdS QDs was slowly added to the mixture solution and stired continuously for 20 min. Finally, the resulting mixtures were collected and washed with deionized water thoroughly. After being dried in vacuum at 400°C for 2 h, the 1 wt% CdS QDs-doped TiO_2 nanocomposites were finally obtained by annealing in air for 2 h at 400–600°C with a heating rate of 2°C/min. For comparison, the pure TiO_2 nanoparticles were prepared by the same method as above, only without adding the corresponding dopants.

The prepared nanoparticles were encapsulated in two bottles, respectively, and subsequently, placed in YX-280B-type pressure steam sterilizer with a high temperature and high pressure (120°C, 1.5 atm) to sterilize for 30 minutes. Finally, an appropriate amount of serum-free medium was added to fully dissolve the nanoparticles. All solutions were filtered through a 0.22 μm membrane filter and stored in the dark at 4°C before being taken into the experiments.

2.3. Cell Culture. Human leukemia HL60 cells were cultured in RPMI 1640 medium supplemented with 10% fetal bovine serum (FBS) in a humidified incubator with 5% CO_2 at 37°C until confluent. The cell concentration was measured using a countess automated cell counter and adjusted to the required final concentration. Cells viability before treatment was always over 95%.

2.4. Cell Viability Assay. The immediate cytotoxicity of the cells after treatment was assessed using the trypan blue exclusion test. The viable/dead cells were counted using a countess automated cell counter. Viability for the samples was further evaluated by Cell Counting Kit-8 assays (CCK-8 assay) [29]. Cell suspension (200 μL) was seeded onto 96-well plate and incubated with 20 μL CCK-8 solution at 37°C in a humidified 5% CO_2 atmosphere. After 4 h incubation, the absorbance (OD values) at 490 nm was determined using the Model 680 Microplate Reader. The percentage of viability was determined by comparison with untreated cells.

2.5. Statistical Analysis. Data are presented as means ± SD (standard deviation) from at least three independent experiments. Statistical analysis is then performed using the statistical software SPSS11.5. Values of $P < 0.05$ are considered statistically significant.

3. Results and Discussion

3.1. Characterization of CdS-TiO_2 Nanocomposites

3.1.1. SEM and TEM Studies. The morphology and particle sizes were observed by a scanning electron microscope. TEM analysis was also performed using a high-resolution transmission electron microscope to obtain further information and support SEM results.

The morphologies of pure TiO_2 and CdS QDs-doped TiO_2 prepared at 400°C are shown in Figure 1. It can be

seen that the average size of pure TiO_2 nanoparticles is significantly larger than that of CdS-TiO_2 nanocomposites. Furthermore, Figures 1(d) and 1(e) display the TEM images and the corresponding size distribution of the CdS-TiO_2, respectively. It appears that the CdS-TiO_2 nanocomposites are spherical or squareshaped with a primary particle size approximately from 17 to 23 nm. This result is consistent with that calculated by the Scherrer equation using the XRD data.

3.1.2. X-Ray Diffraction. XRD was used to further investigate the crystalline structural properties of CdS-doped TiO_2, and the XRD patterns are presented in Figure 2. Figure 2 illustrates that the principal peaks, which are consistent with crystalline phases of (101), (004), (200), (105), and (211), were found in both TiO_2 nanoparticles and CdS-TiO_2 nanocomposites, indicating that the samples obtained by the sol-gel method have primarily the anatase phase. Meanwhile, there are no indications of peaks corresponding to CdS; it may be attributed to that the amount of CdS is small and dispersed well into the TiO_2. Additionally, compared with that of TiO_2, no significant shift of principal peaks of the CdS-TiO_2 is observed, further confirming that the samples prepared here are highly crystallized, which is essential for a good photocatalytic material.

According to the Scherrer's formula ($D = k\lambda/\beta\cos\theta$, $k = 0.89$, $\lambda = 0.15418$ nm, $2\theta = 25.4^\circ$ for anatase phase), it is calculated that the average crystallite sizes are 21.5 nm and 19.3 nm for TiO_2 nanoparticles and CdS-TiO_2 nanocomposites, respectively. These results reveal that the incorporation of CdS QDs could effectively inhibit the crystallite growth, which are basically consistent with the TEM results shown in Figure 1.

3.1.3. UV-vis Spectroscopy. The CdS-TiO_2 nanocomposites have been identified with UV-Vis adsorption spectra. As is shown in Figure 3, the controlled TiO_2 could absorb mainly the ultraviolet light with wavelength below 400 nm due to its intrinsic band gap of anatase-TiO_2 (3.2 eV). However, compared with those of the undoped TiO_2, the absorption edge thresholds of the CdS-TiO_2 are distinctly shifted towards the visible region for the narrow band gap of CdS (2.4 eV). Additionally, Figure 3 also exhibits that the onset of the absorption spectrum of CdS-TiO_2 is extended from 395 nm to visible range 427 nm. According to the formula $\lambda = 1240/E_g$ [22], the band gap energy of the TiO_2 and CdS-TiO_2 are 3.15 eV and 2.92 eV, respectively. These results confirm that the absorption of visible light of TiO_2 nanoparticles has been effectively enhanced by the incorporation of CdS QDs, which is beneficial for improving the photocatalytic activity of TiO_2.

In order to reach a high photocatalytic inactivation efficiency, an in-house built lamp with many high-power light-emitting diodes (LEDs), emitting light in the visible-light region 390–425 nm and with a peak at 403.25 nm, was taken as light sources for PDT in the experiments. The light density at the position of the sample was 5 mW/cm^2 as measured with a photodiode. As shown in the inserting graph, the blue LEDs can better meeting the needs of PDT experiments.

3.1.4. EDS Analysis. In order to confirm the formation of CdS quantum dots and successfully incorporate them into CdS-TiO_2 nanocomposites (QDs), the prepared CdS-TiO_2 sample was investigated using energy dispersive X-ray spectroscopy analysis. As it can be observed from Figure 4, the observed peaks of Cd and S are evidence that the CdS QDs have been doped into TiO_2 to form the CdS-TiO_2 nanocomposites. Moreover, EDS analysis also shows the presence of Cd and S are 0.86 at% and 0.91 at%, respectively, which are consistent with theoretical values and further confirming the stoichiometric formation of CdS.

3.1.5. FS Analysis. The efficiency of photocatalytic activity and charge trapping in the semiconductor could be verified by FS spectra [30]. As can be seen from Figure 5, the intensity of the fluorescence peak of CdS-TiO_2 nanocomposites at 700 nm is much weaker than that of TiO_2 nanoparticles. The fluorescence emission of semiconductor is mainly caused by the recombination of photoinduced electrons and holes. Therefore, the doping of CdS could effectively separate photoinduced electrons from holes on the surface of TiO_2 thus inhibit their recombination, resulting in enhanced photocatalytic activity.

3.1.6. Photocatalytic Performance. The photocatalytic activities of the controlled TiO_2 and CdS-doped TiO_2 samples were evaluated by the degradation of methyl orange under visible-light irradiation. In the experiment, 250 mg of CdS-TiO_2 was dispersed in 250 mL of methyl orange solutions (5 mg/L) to obtain the concentration of photocatalyst at 1.0 g/L. Before irradiation, the suspension was stirred in the dark at room temperature for 0.5 h to reach the absorption-desorption equilibrium of the dye molecules on the sample surface. 3 mL of the solution was collected at irradiation time intervals of 10 min then centrifuged (5000 rpm, 15 min) to remove the photocatalyst particles. The sample solution was finally analyzed with a Hitachi UV-3010 UV-vis spectrophotometer.

The photocatalytic degradation curves of methyl orange under irradiation in the presence of the controlled TiO_2 or CdS that doped TiO_2 are shown in Figure 6. It exhibits methyl orange in the absence of any catalyst under visible-light irradiation only has a very weak degradation compared with the situation of adding catalysts. However, the concentration of methyl orange is decreased significantly at the average decline rate of approximately 3.7% every 10 minute in the presence of TiO_2, which is similar to the linear decline. Compared with that of the controlled TiO_2, the normalized concentration of methyl orange with CdS-TiO_2 is decreasing exponentially during light exposure. It is also found that the concentration of methyl orange in the presence of CdS-TiO_2 has decreased by 67.5% after 70-minute light treatment as compared to values before the treatment, suggesting that the CdS QDs-doped TiO_2 exhibits much higher photocatalytic activity than TiO_2 under visible-light irradiation.

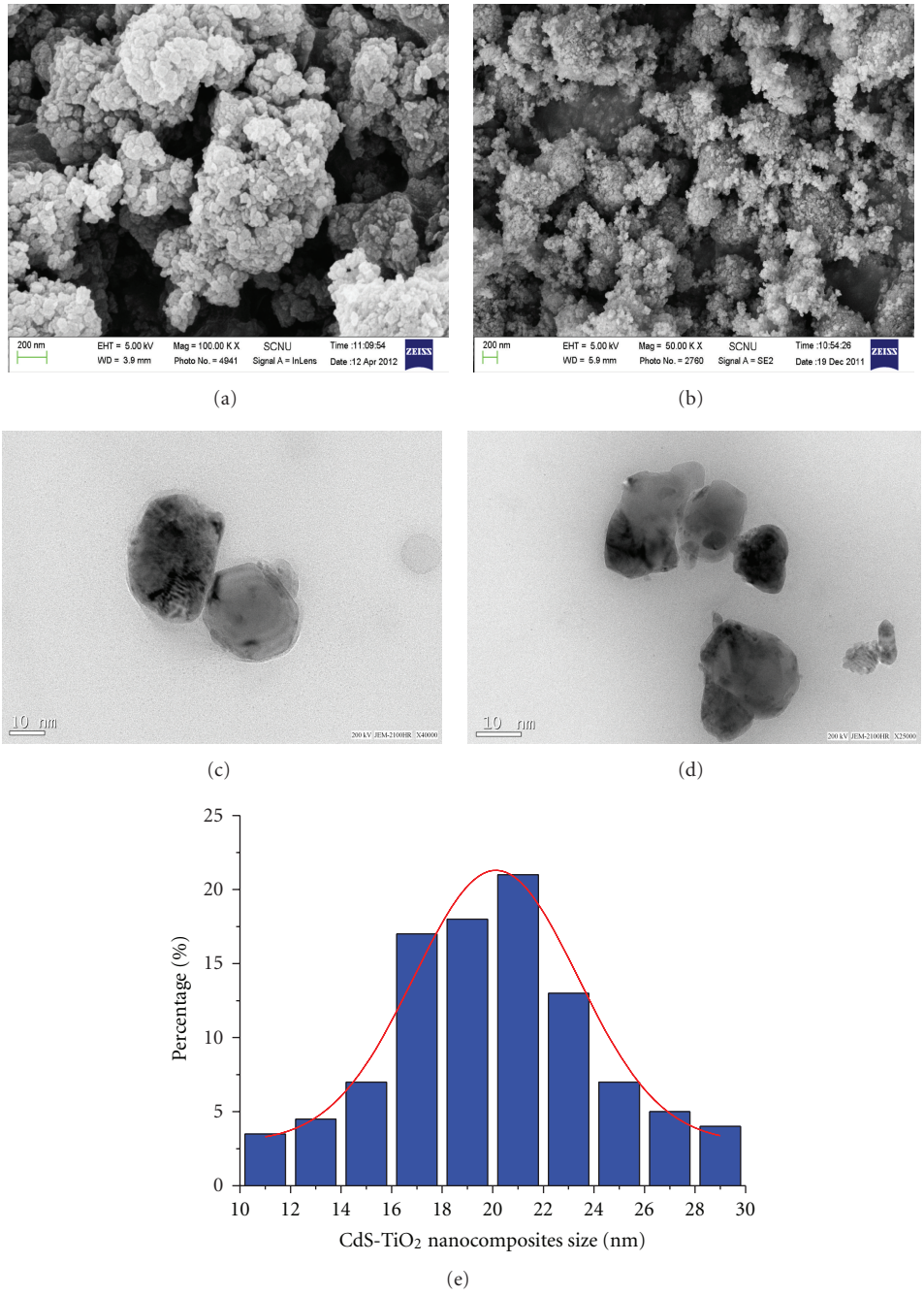

Figure 1: SEM and TEM images of TiO_2 and CdS-TiO_2 nanocomposites: (a) and (c) pure TiO_2; (b) and (d) CdS-TiO_2; (e) size distribution of CdS/TiO_2 nanocomposites.

3.2. Cytotoxicity of TiO_2 or CdS-TiO_2 Alone on Leukemia Tumor Cells. HL60 cells in the logarithmic phase at a final concentration of 1×10^5 cells/mL were seeded into 96-well culture plates which had been divided into 3 groups, namely, the control group, TiO_2 group, and the CdS-TiO_2 group, respectively. The OD values (which is used to determine the cell viability by comparison with untreated cells) of the samples in the presence of 200 μg/mL TiO_2 or CdS-TiO_2 were measured by Model 680 Microplate Reader for 6 consecutive days without adding nutrients. The experimental data are presented in Figure 7.

As can be seen from Figure 7, all HL60 cells of the three groups show a low growth rate on the first day, indicating they are in the adaptation period. However, the growth rate of the HL60 cells increased rapidly exponentially during the next three days. In this study, the cells during this period are used in all experiments. On the fifth day, the growth rate of cells become more slowly and stabilized down gradually.

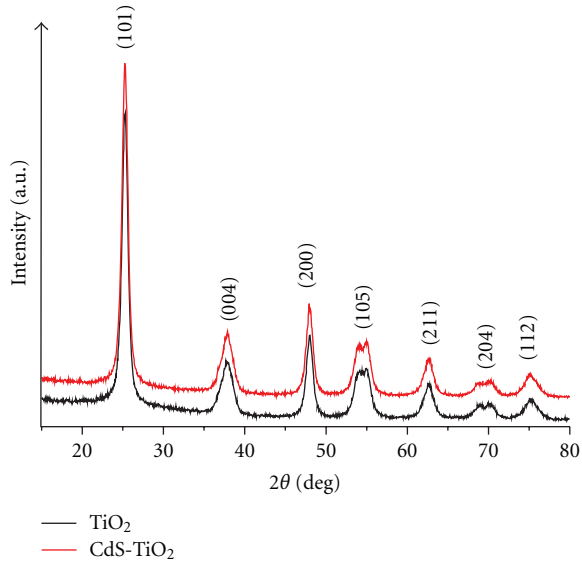

Figure 2: XRD patterns of TiO_2 nanoparticles and CdS-doped TiO_2 nanocomposites calcined at 400°C.

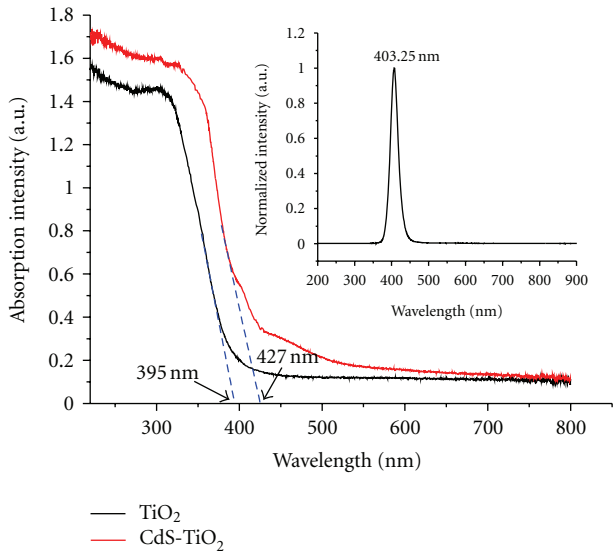

Figure 3: UV-Vis absorption spectra of TiO_2 and CdS-TiO_2 samples; inset is the normalized emission spectra of the blue LEDs.

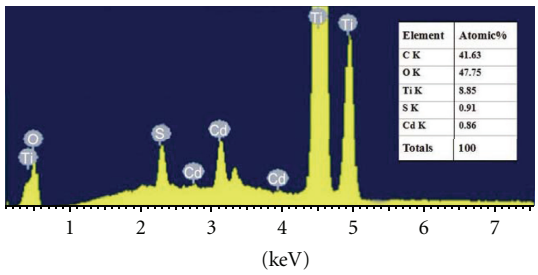

Figure 4: EDS spectra of CdS-TiO_2 nanocomposites calcined at 400°C.

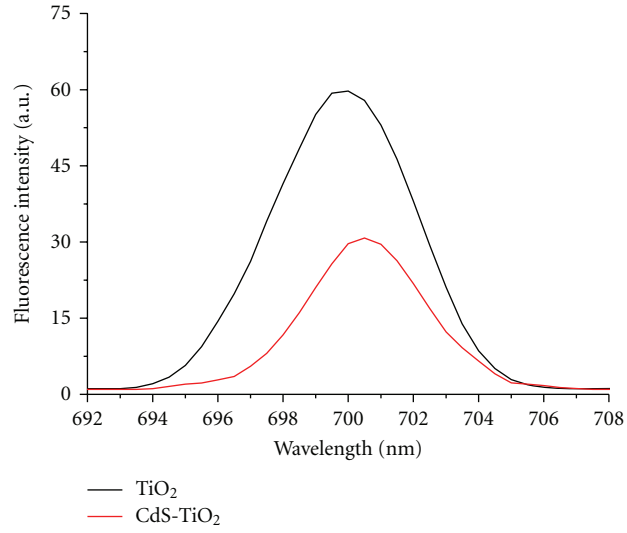

Figure 5: Fluorescence spectra of TiO_2 and CdS-TiO_2 samples with the excitation wavelength of 350 nm.

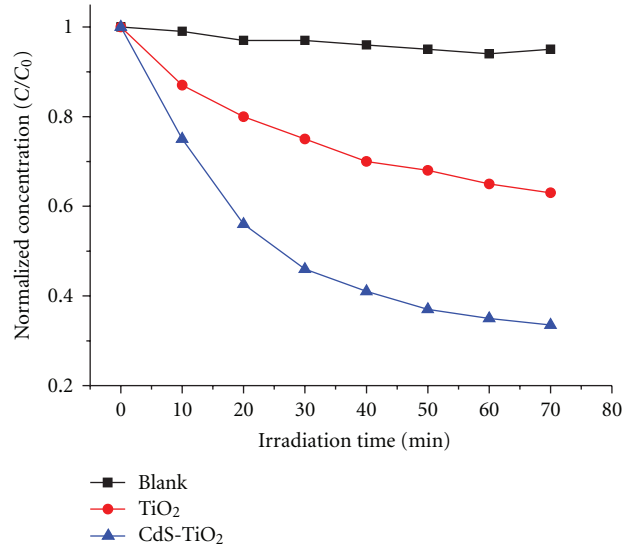

Figure 6: Photodegradation of methyl orange with TiO_2 and CdS-TiO_2 samples under visible-light irradiation.

Additionally, the number of viable cells started to decrease from the sixth day due to the continuous depletion of nutrients and the accumulation of toxic metabolites.

Figure 7 also exhibits that OD values of the groups in the presence of TiO_2 or CdS-TiO_2 are much lower and with a shorter growth phase than that of the control group under the same conditions. The results reveal that TiO_2 or CdS-TiO_2 has a certain degree of inhibitory or cytotoxicity on the proliferation of HL60 cells. Moreover, the inhibition effect of CdS-TiO_2 nanocomposites on HL60 cells is much more obvious than that of TiO_2.

3.3. Influence of Nanoparticle Concentration and Light Dose on Phototoxicity. The influence of nanoparticle concentration

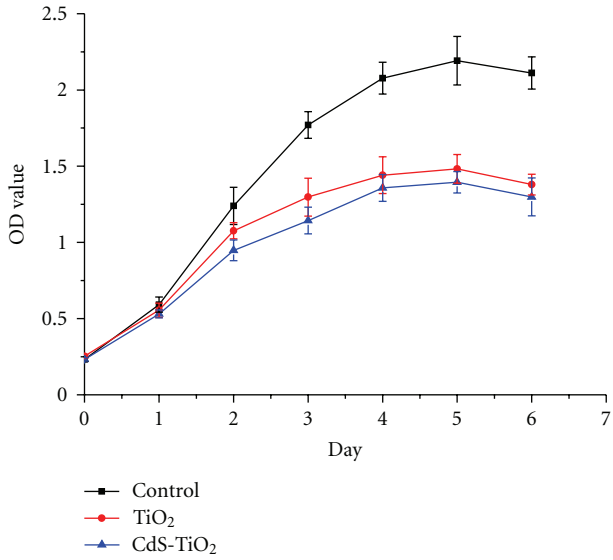

Figure 7: Influence of nanoparticles on the proliferation of HL60 cells; data represent the means ± S.D. ($n = 3$), $^*P < 0.05$.

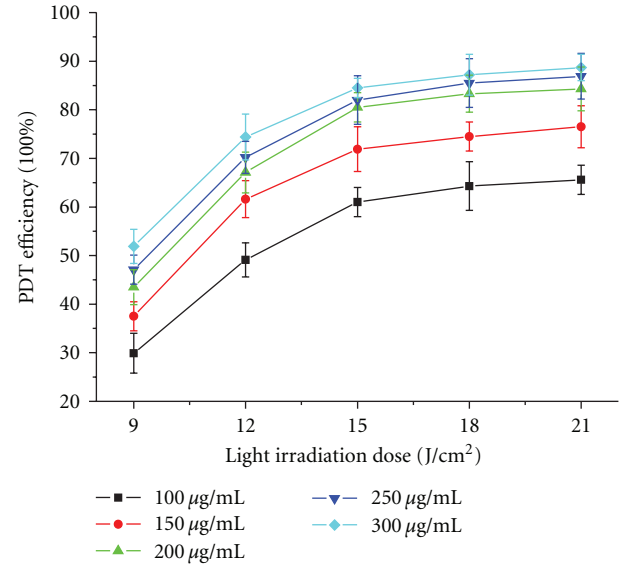

Figure 8: Influence of CdS-TiO_2 nanocomposites concentration and light dosage on the PDT efficiency of HL60 cells; data are presented as the means ± S.D. from three independent measurements, $^*P$ values are less than 0.05 as compared with untreated control cells.

and light dosage was measured by exposing HL60 cells in the medium containing various concentrations of CdS-TiO_2 (100 μg/mL, 150 μg/mL, 200 μg/mL, 250 μg/mL, and 300 μg/mL) under series of light dosage (9 J/cm^2, 12 J/cm^2, 15 J/cm^2, 18 J/cm^2, and 21 J/cm^2), respectively. The photocatalytic effects of CdS-TiO_2 nanocomposites on leukemic HL60 cells were evaluated by measuring OD values, and PDT efficiency could be calculated as follows:

$$\text{PDT efficiency (\%)} = \left(1 - \frac{\text{OD}_{\text{treated}}}{\text{OD}_{\text{untreated}}}\right) \cdot 100\%, \quad (1)$$

where the $\text{OD}_{\text{treated}}$ and $\text{OD}_{\text{untreated}}$ are the mean absorption values at 490 nm for the treated and untreated samples, respectively. The obtained results are summarized in Figure 8.

As shown in Figure 8, the inactivation PDT efficiency of CdS-TiO_2 nanocomposites on HL60 cells is significantly increased with the increasing of light dose under the same concentration of nanoparticles solution, whereas the increasing effects of PDT are not obviously when the dosage of irradiation is greater than 15 J/cm^2. Furthermore, light dose is too large which will also inevitably lead to a greater damage to normal cells, which is in agreement with the suggestions reported [31, 32]. Figure 8 also exhibits that photodynamic effect of CdS-TiO_2 is obviously enhanced with the increasing of the concentration of CdS-TiO_2 nanocomposites under the same light dose. However, when the concentration of CdS-TiO_2 is more than 200 μg/mL, PDT efficiency is not significantly different ($P > 0.05$). Therefore, the light dose of 15 J/cm^2 and the concentration of 200 μg/mL in this case are regarded as the optimized parameters for the experiments.

3.4. Photocatalytic Inactivation Effects of CdS-TiO_2 Nanocomposites on Cancer Cells under the Optimal Parameters. As can be observed in Figure 9, when the cells were treated with TiO_2 alone or light irradiation alone, PDT efficiency showed no significant differences as compared with untreated ones. However, cells treated with the combination of TiO_2 and light exposure resulted in a significant increase in PDT efficiency. It can also be found that the PDT efficiency of HL60 cells in the presence of CdS-TiO_2 is much higher than that of TiO_2 under light irradiation. These results have well demonstrated that the incorporation of CdS QDs could significantly enhance the photocatalytic inactivation effect of TiO_2 under visible-light irradiations. Additionally, the CdS-TiO_2 nanocomposites exhibit a higher efficiency in photokilling HL60 cancer cells compared with that of TiO_2 samples under the same conditions. When 200 μg/mL CdS-TiO_2 nanocomposites were used, the inactivation efficiency of HL60 Cells can be increased to 80.5% under 403 nmlight treatment.

3.5. Ultrastructural Morphology of Cells before or after PDT

3.5.1. SEM Studies. After light treatment (PDT), the treated cells were immediately fixed in 2.5% glutaraldehyde in 0.1 M phosphate buffer (pH 7.2) for 8 h. They were then washed three times thoroughly with triple-distilled water and dehydrated in an ethanol-graded series (30%, 50%, 70%, 80%, 90%, 100%) each for 10 minutes before being freeze-dried using K750 turbo freeze drier. The samples were coated with platinum using automatic high vacuum coating system (Quorum Q150T ES) before observing with a ZEISS Ultra-55 scanning electron microscope.

The ultrastructural morphology of the HL60 cells exposed to light at an intensity of 5.0 mW/cm^2 for 50 minutes in the presence CdS-TiO_2nanocomposites is shown

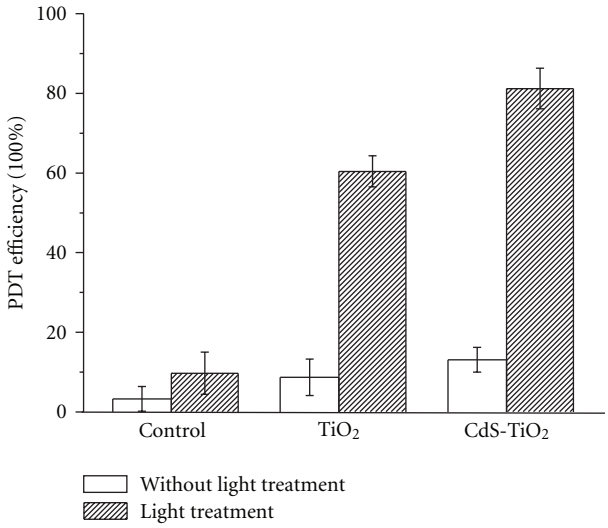

Figure 9: PDT efficiency of HL60 cells in the presence of TiO_2 or CdS-TiO_2 under the optimal parameters (15 J/cm^2, 200 μg/mL); Each data point represents mean ± S.D. ($n = 3$), $^*P < 0.05$.

in Figure 10. Untreated control cells with a primary size of 10 μm showed numerous microvilli on their membrane surface (Figure 10(a)). The cells treated with CdS-TiO_2 alone showed a significant reduction of microvilli number (Figure 10(b)). The cells exposed with 403 nm light in the absence of CdS-TiO_2 displayed no obvious differences compared with those treated with CdS-TiO_2 alone (Figure 10(c_1)). However, the cells exposed to light in the presence of CdS-TiO_2 nanocomposites displayed a markedly reduced number of microvilli compared with control cells (Figure 10(d_1)). The treated cells after PDT were seriously damaged with apparent deformation. Some papillous protuberances are observed on the surface of cells where the cytoplasm seemed to have extruded through the membrane boundary.

According to the high-definition images of control cells and the cells after PDT in Figures 10(c_2) and 10(d_2) respectively, The control cells showed a good compactness cell membrane, whereas the cell membrane after PDT was severely deformed and a lot of micropores could be observed on the surface of cell membrane. It can be interpreted that the generated reactive oxygen species firstly caused oxidative damage to cell membranes of tumor cells, making the cell membrane permeability change. Then the smaller size of CdS-TiO_2 nanocomposites may be swallowed or diffusion into the cells directly attack the composition of cells, eventually leading to tumor cell death [33, 34].

3.5.2. AMF Analysis. AMF analysis was also performed using a high-resolution atomic force microscopy (AFM) to obtain further information and support SEM results. After light treatment (PDT), the treated cells were immediately fixed in 2.5% glutaraldehyde in 0.1 M phosphate buffer (pH 7.2) for 2 h. They were then washed three times thoroughly with triple-distilled water and reproduced with an appropriate volume of PBS. Afterwards, the cell solution was added dropwise to the coverslips which have been cleaned with distilled water (the size of coverslips is matched with the AFM sample stage). Finally, the liquid was dried naturally at room temperature before imaging.

As can be seen from Figure 11(a_1) and local amplification Figure 11(a_2), the controlled HL60 cells with a size of 10 μm show a cylindrical shape and numerous microvilli on their bright surface. In addition, surface roughness analysis (Figure 11(a_3)) shows that the normal cells with a smooth surface (average roughness in the range from 5 to 10 nm).

Figures 11(b_1) and 11(b_2) exhibit that the cells treated with CdS-TiO_2 nanocomposites under visible-light irradiation become irregular in shape and the cell size (9.3 μm) is smaller than that of control cells. The smooth membrane surface has been completely destroyed and become rough and uneven. Additionally, a large quantity of bubbles as well as cell cracks can be observed on enlarged cell surface (Figure 11(b_2)). The obtained results reveal that the cell membrane should be the first and principal target of photosensitization reaction in PDT based on CdS-TiO_2 induced-cell death. Furthermore, Figure 11(b_3) illustrates the roughness of the cell surfaces with variations in height up to 80 nm.

3.6. Apoptosis Detection Based on the Induction of CdS-TiO_2. The percentage of apoptotic cells after PDT was investigated by the number and sizes of dead cell obtained from the Cell Counter in combination with the nondestructive testing methods [35].

The obtained data are shown in Figure 12; no significant difference of the number of apoptotic cells is obtained with light treatment alone or CdS-doped TiO_2 alone compared with control untreated cells. The percentage of apoptotic cells in the presence of CdS-doped TiO_2 after a 15 W/cm^2 light treatment is 10.3 times greater than that of control untreated cells. It is suggested that CdS-TiO_2 nanocomposites-induced cell death is mainly caused by apoptosis.

3.7. Alteration of ROS HL60 Cells during PDT. Related studies have well established that reactive oxygen species (ROS) not only could directly damage the membrane of cells through oxidation of critical cellular macromolecules, but also could act as important signaling molecules. The generation of ROS may be one of the most important signatures of cytotoxicity induced by TiO_2 nanoparticles, which is similar to those described [36, 37].

The changes of the reactive oxygen species during light treatment were detected by reactive oxygen species assay. Firstly, DCFH-DA was diluted with serum-free media to a final concentration of 10 μM. Subsequently, an appropriate volume of the prepared solution was added to the treated cells and then incubated for 20 minutes. Finally, they were washed three times with PBS to remove the DCFH-DA did not enter the cells before being detected using fluorescence spectrophotometer (an excitation wavelength at 486 nm, and emission wavelength from 517 to 700 nm). The obtained results are presented in Figure 13.

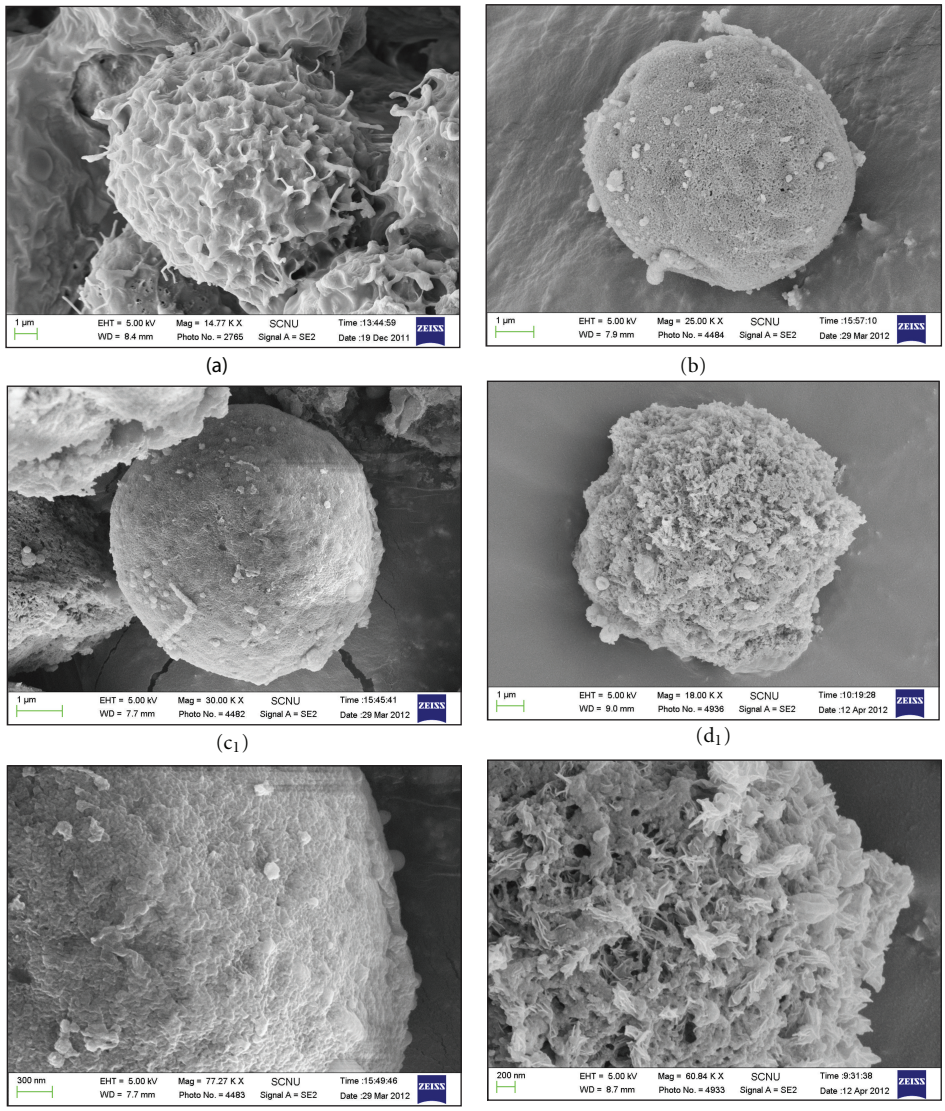

Figure 10: Ultrastructural morphology of the treated HL60 cells. (a: The control cells, b: cells treated with CdS-TiO_2, c: The light treated cells, d: The cells after PDT).

The cells were incubated with CdS-TiO_2 nanocomposites at a final concentration 200 μg/mL for 4 h; then irradiated with 403 nm light at intensity of 5 mW/cm^2. Figure 13(a) illustrates alteration of ROS during PDT. It can be found that the level of intracellular reactive oxygen species increased rapidly at the beginning of 10 minutes and reached the maximum after 30-minute light treatment (as shown in Figure 13(b)). After that, the generated reactive oxygen species began to decline slowly. Compared with the previous PDT experiments, it can be found that the PDT efficiency could be indirectly characterized by changes in the concentration of reactive oxygen species.

3.8. Mechanism of Photocatalysis on CdS-TiO_2 Nanocomposites. It has been reported that the dopant elements play an important role in the photocatalytic activity of TiO_2 catalyst by trapping the photo-induced electrons to inhibit electron-hole recombination during irradiation, as suggested [38, 39].

The photocatalytic mechanism of CdS-TiO_2 nanocomposites is initiated by the absorption of a photon with energy higher than the band gap of CdS-TiO_2 as schematized in Scheme 1. Afterwards, photo-induced electrons and holes could be generated on the surfaces of CdS and TiO_2. Since to both the conduction band (CB) and the valence band (VB) of CdTe QDs are above those of TiO_2, the generated electrons in CdS are then promoted to the conduction band (CB) of TiO_2 under a driving force that resulted from the different energy levels. Meanwhile, the holes in TiO_2 are immigrated toward the valence band (VB) of CdS. On the one hand, the excited-state electrons probably reduce the

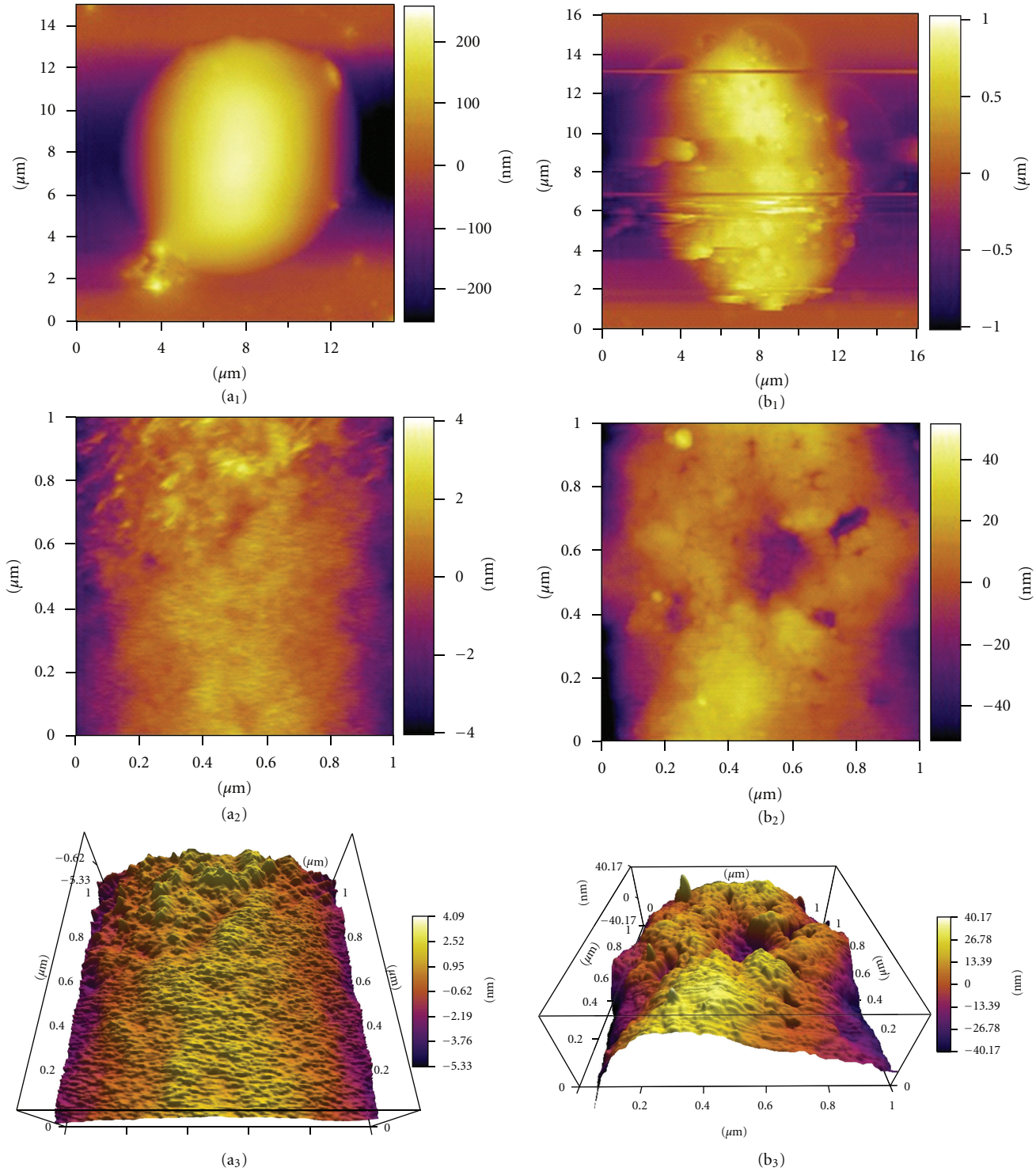

Figure 11: Ultrastructural morphology of the cultured HL60 cells before and after PDT. (a): The control cells, (b): the treated cells.

dissolved O_2 to produce oxygen peroxide O^-. On the other hand, the photogenerated holes can further react with water to generate powerful hydroxyl radicals ($OH^\bullet$) and other oxidative radicals, which are playing an important role in destroying the membrane and component of tumor cells [40, 41]. Additionally, the efficient charge transfer could effectively separate photo-induced electrons from holes in the CdS-TiO_2 and thus inhibit their recombination, resulting

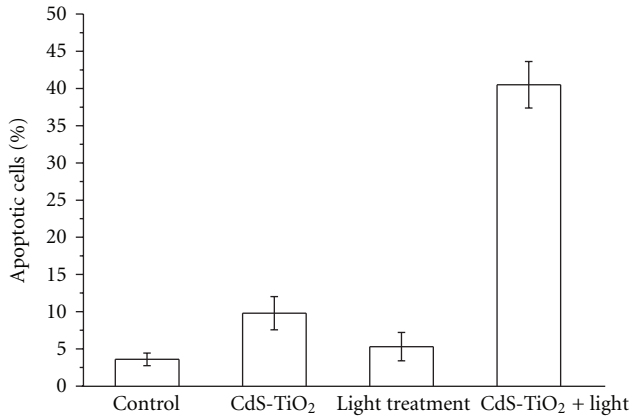

Figure 12: Change of percentage of apoptotic cells after PDT; each data point represents mean ± S.D. ($n = 3$), $^*P < 0.05$.

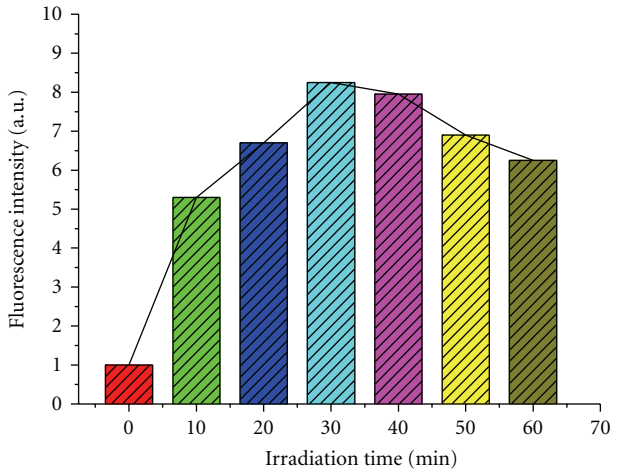

(a)

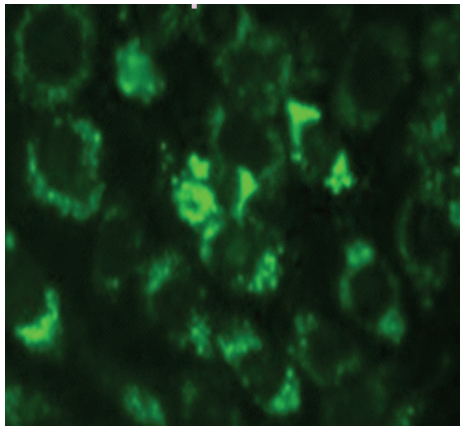

(b)

Figure 13: (a) Alteration of ROS in HL60 cells after 4 h incubation with CdS-TiO_2 nanocomposites during PDT, $^*P < 0.05$; (b) the intracellular ROS after 30-minutes light treatment.

in significantly enhanced quantum efficiency and facilitating the formation of active radicals [42, 43]. Regardless of

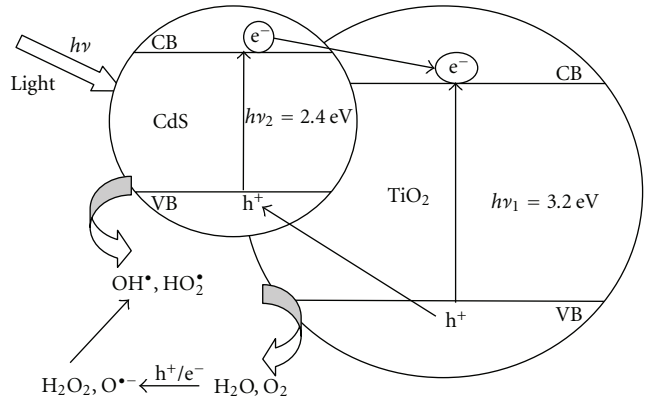

Scheme 1: Schematic representation of the mechanism of excitation and charge transfer process between CdS and TiO_2 in the CdS-TiO_2 nanocomposites under irradiation.

complexity, it is apparent that there are several photosensitive keys involved which could be also explained as follows:

$$
\begin{aligned}
&TiO_2 \xrightarrow{h\nu} TiO_2(e^- \cdots h^+)\\
&H_2O + h^+ \longrightarrow OH^\bullet + H^+\\
&O_2 + e^- \longrightarrow O_2^\bullet \longrightarrow HO_2^\bullet\\
&2HO_2^\bullet \longrightarrow O_2 + H_2O_2\\
&H_2O_2 + O_2^\bullet \longrightarrow OH^\bullet + OH^- + O_2\\
&CdS \xrightarrow{h\nu} CdS(e^- \cdots h^+)\\
&CdS(e^- \cdots h^+) + TiO_2 \longrightarrow CdS(h^+) + TiO_2(e^-)
\end{aligned}
\tag{2}
$$

4. Conclusion

In this study, CdS-TiO_2 nanocomposites have been successfully synthesized by sol-gel approach and for the first time used as a new "photosensitizer" in photodynamic therapy for cancer-cell treatment. Results of various characterization techniques indicate that the incorporation of CdS QDs into TiO_2 nanoparticles can effectively extend the photoresponse of the undoped TiO_2 into the visible region and improve the charge separation efficiency thus enhancing the photocatalytic activity. Additionaly, relevant experiments have demonstrated that both pure TiO_2 and CdS-TiO_2 nanocomposites have a significant inhibition effect on the growth of HL60 cells. CdS-TiO_2 nanocomposites present much higher PDT efficiency in photo-killing HL60 cancer cells than TiO_2 nanoparticles under the same conditions, which further reveal that the photocatalytic inactivation effects of TiO_2 could be greatly improved by the modification of CdS QDs. It is also found that the PDT efficiency of CdS-TiO_2 nanocomposites on HL60 cells can reach 80.5% at a concentration of 200 μg/mL under a 15 J/cm^{2}light treatment. The high photocatalytic inactivation effect of CdS-TiO_2 nanocomposites on cancer cells suggests that it may be

an important potential photosensitizer-based photodynamic therapy for malignant cancer treatment [44–46].

Acknowledgments

This work has been financially supported by National Natural Science Foundation of China (61072029), Natural Science Foundation of Guangdong Province (10151063101000025), and Science and Technology Planning Project of Guangzhou City (2010Y1-C111).

References

[1] M. R. Hoffmann, S. T. Martin, W. Choi, and D. W. Bahnemann, "Environmental applications of semiconductor photocatalysis," *Chemical Reviews*, vol. 95, no. 1, pp. 69–96, 1995.

[2] J. Xu, Y. Sun, J. Huang et al., "Photokilling cancer cells using highly cell-specific antibody-TiO_2 bioconjugates and electroporation," *Bioelectrochemistry*, vol. 71, no. 2, pp. 217–222, 2007.

[3] J. Yu, Q. Xiang, and M. Zhou, "Preparation, characterization and visible-light-driven photocatalytic activity of Fe-doped titania nanorods and first-principles study for electronic structures," *Applied Catalysis B*, vol. 90, no. 3-4, pp. 595–602, 2009.

[4] J. A. Byrne, P. A. Fernandez-Ibañez, P. S. M. Dunlop, D. M. A. Alrousan, and J. W. J. Hamilton, "Photocatalytic enhancement for solar disinfection of water: a review," *International Journal of Photoenergy*, vol. 2011, Article ID 798051, 12 pages, 2011.

[5] K. Lv, J. Li, X. Qing, W. Li, and Q. Chen, "Synthesis and photodegradation application of WO_3/TiO_2 hollow spheres," *Journal of Hazardous Materials*, vol. 189, no. 1-2, pp. 329–335, 2011.

[6] Q. Xiang, J. Yu, and P. K. Wong, "Quantitative characterization of hydroxyl radicals produced by various photocatalysts," *Journal of Colloid and Interface Science*, vol. 357, no. 1, pp. 163–167, 2011.

[7] M. Mrowetz, W. Balcerski, A. J. Colussi, and M. R. Hoffmann, "Oxidative power of nitrogen-doped TiO_2 photocatalysts under visible illumination," *Journal of Physical Chemistry B*, vol. 108, no. 45, pp. 17269–17273, 2004.

[8] J. Wang, Y. Guo, B. Liu et al., "Detection and analysis of reactive oxygen species (ROS) generated by nano-sized TiO_2 powder under ultrasonic irradiation and application in sonocatalytic degradation of organic dyes," *Ultrasonics Sonochemistry*, vol. 18, no. 1, pp. 177–183, 2011.

[9] J. J. Wang, B. J. S. Sanderson, and H. Wang, "Cyto- and genotoxicity of ultrafine TiO_2 particles in cultured human lymphoblastoid cells," *Mutation Research*, vol. 628, no. 2, pp. 99–106, 2007.

[10] Y. S. Lee, S. Yoon, H. J. Yoon et al., "Inhibitor of differentiation 1 (Id1) expression attenuates the degree of TiO_2-induced cytotoxicity in H1299 non-small cell lung cancer cells," *Toxicology Letters*, vol. 189, no. 3, pp. 191–199, 2009.

[11] K. Huang, L. Chen, J. Xiong, and M. Liao, "Preparation and characterization of visible-light-activated Fe-N Co-doped TiO_2 and its photocatalytic inactivation effect on leukemia tumors," *International Journal of Photoenergy*, vol. 2012, Article ID 631435, 9 pages, 2012.

[12] F. Wei, H. Zeng, P. Cui, S. Peng, and T. Cheng, "Various TiO_2 microcrystals: controlled synthesis and enhanced photocatalytic activities," *Chemical Engineering Journal*, vol. 144, no. 1, pp. 119–123, 2008.

[13] X. Chen and S. S. Mao, "Titanium dioxide nanomaterials: synthesis, properties, modifications and applications," *Chemical Reviews*, vol. 107, no. 7, pp. 2891–2959, 2007.

[14] J. Yu, G. Dai, Q. Xiang, and M. Jaroniec, "Fabrication and enhanced visible-light photocatalytic activity of carbon self-doped TiO_2 sheets with exposed 001 facets," *Journal of Materials Chemistry*, vol. 21, no. 4, pp. 1049–1057, 2011.

[15] H. Li, Z. Bian, J. Zhu, Y. Huo, H. Li, and Y. Lu, "Mesoporous Au/TiO_2 nanocomposites with enhanced photocatalytic activity," *Journal of the American Chemical Society*, vol. 129, no. 15, pp. 4538–4539, 2007.

[16] V. Iliev, D. Tomova, R. Todorovska et al., "Photocatalytic properties of TiO_2 modified with gold nanoparticles in the degradation of oxalic acid in aqueous solution," *Applied Catalysis A*, vol. 313, no. 2, pp. 115–121, 2006.

[17] R. Bacsa, J. Kiwi, T. Ohno, P. Albers, and V. Nadtochenko, "Preparation, testing and characterization of doped TiO_2 active in the peroxidation of biomolecules under visible light," *Journal of Physical Chemistry B*, vol. 109, no. 12, pp. 5994–6003, 2005.

[18] J. A. Rengifo-Herrera and C. Pulgarin, "Photocatalytic activity of N, S co-doped and N-doped commercial anatase TiO_2 powders towards phenol oxidation and E. coli inactivation under simulated solar light irradiation," *Solar Energy*, vol. 84, no. 1, pp. 37–43, 2010.

[19] M. Zhou, J. Zhang, B. Cheng, and H. Yu, "Enhancement of visible-light photocatalytic activity of mesoporous Au-TiO_2 nanocomposites by surface plasmon resonance," *International Journal of Photoenergy*, vol. 2012, Article ID 532843, 10 pages, 2012.

[20] H. Choi, E. Stathatos, and D. D. Dionysiou, "Sol-gel preparation of mesoporous photocatalytic TiO_2 films and TiO_2/Al_2O_3 composite membranes for environmental applications," *Applied Catalysis B*, vol. 63, no. 1-2, pp. 60–67, 2006.

[21] K. Lv, J. Yu, K. Deng, X. Li, and M. Li, "Effect of phase structures on the formation rate of hydroxyl radicals on the surface of TiO_2," *Journal of Physics and Chemistry of Solids*, vol. 71, no. 4, pp. 519–522, 2010.

[22] Y. S. Li, F. L. Jiang, Q. Xiao et al., "Enhanced photocatalytic activities of TiO_2 nanocomposites doped with water-soluble mercapto-capped CdTe quantum dots," *Applied Catalysis B*, vol. 101, no. 1-2, pp. 118–129, 2010.

[23] P. Juzenas, W. Chen, Y. P. Sun et al., "Quantum dots and nanoparticles for photodynamic and radiation therapies of cancer," *Advanced Drug Delivery Reviews*, vol. 60, no. 15, pp. 1600–1614, 2008.

[24] J. Yu, J. Zhang, and M. Jaroniec, "Preparation and enhanced visible-light photocatalytic H2- production activity of CdS quantum dots-sensitized $Zn_{1-x}Cd_xS$ solid solution," *Green Chemistry*, vol. 12, no. 9, pp. 1611–1614, 2010.

[25] A. Maurya and P. Chauhan, "Structural and optical characterization of CdS/TiO_2 nanocomposite," *Materials Characterization*, vol. 62, no. 4, pp. 382–390, 2011.

[26] R. Wang, D. Xu, J. Liu, K. Li, and H. Wang, "Preparation and photocatalytic properties of $CdS/La_2Ti_2O_7$ nanocomposites under visible light," *Chemical Engineering Journal*, vol. 168, no. 1, pp. 455–460, 2011.

[27] U. G. Akpan and B. H. Hameed, "The advancements in sol-gel method of doped-TiO_2 photocatalysts," *Applied Catalysis A*, vol. 375, no. 1, pp. 1–11, 2010.

[28] N. Gaponik, D. V. Talapin, A. L. Rogach et al., "Thiol-capping of CDTe nanocrystals: an alternative to organometallic synthetic routes," *Journal of Physical Chemistry B*, vol. 106, no. 29, pp. 7177–7185, 2002.

[29] J. W. Xiong, H. Xiao, L. Chen, J. M. Wu, and Z. X. Zhang, "Research on different detection conditions between MTT and CCK-8," *Acta Laser Biology Sinica*, vol. 16, no. 5, pp. 526–531, 2007.

[30] J. Liqiang, Q. Yichun, W. Baiqi et al., "Review of photoluminescence performance of nano-sized semiconductor materials and its relationships with photocatalytic activity," *Solar Energy Materials and Solar Cells*, vol. 90, no. 12, pp. 1773–1787, 2006.

[31] Z. X. Zhang, S. J. Zhang, B. Q. Zhang, and M. L. Chen, "Leukemic cells killed by photodynamic therapy with 5-aminolevulinic acid: an experimental study," *Chinese Journal of Laser Medicine & Surgery*, vol. 14, no. 4, pp. 249–252, 2005.

[32] H. Xiao, J. W. Xiong, J. M. Wu, and Z. X. Zhang, "Research of parameters on ALA-PDT destruction of leukaemie cell," *Acta Laser Biology Sinica*, vol. 13, no. 5, pp. 353–357, 2004.

[33] N. P. Huang, M. H. Xu, C. W. Yuan, and R. R. Yu, "The study of the photokilling effect and mechanism of ultrafine TiO_2 particles on U937 cells," *Journal of Photochemistry and Photobiology A*, vol. 108, no. 2-3, pp. 229–233, 1997.

[34] J. F. Reeves, S. J. Davies, N. J. F. Dodd, and A. N. Jha, "Hydroxyl radicals ($\cdot$OH) are associated with titanium dioxide (TiO_2) nanoparticle-induced cytotoxicity and oxidative DNA damage in fish cells," *Mutation Research*, vol. 640, no. 1-2, pp. 113–122, 2008.

[35] J.-W. Xiong, L. Chen, M.-S. Liu et al., "Optical manner for estimation viability of cells based on their morphological characteristics," *Journal of Optoelectronics Laser*, vol. 16, no. 12, pp. 1514–1519, 2005.

[36] K. Huang, L. Chen, M. Liao, and J. Xiong, "The photocatalytic inactivation effect of Fe-doped TiO_2 nanocomposites on leukemic HL60 cells-based photodynamic therapy," *International Journal of Photoenergy*, vol. 2012, Article ID 367072, 8 pages, 2012.

[37] C. M. Sayes, R. Wahi, P. A. Kurian et al., "Correlating nanoscale titania structure with toxicity: a cytotoxicity and inflammatory response study with human dermal fibroblasts and human lung epithelial cells," *Toxicological Sciences*, vol. 92, no. 1, pp. 174–185, 2006.

[38] X. Zhou, J. Lu, L. Li, and Z. Wang, "Preparation of crystalline Sn-Doped TiO_2 and its application in visible-light photocatalysis," *Journal of Nanomaterials*, vol. 2011, Article ID 432947, 5 pages, 2011.

[39] Q. Kang, Q. Z. Lu, S. H. Liu et al., "A ternary hybrid CdS/Pt-TiO_2 nanotube structure for photoelectrocatalytic bactericidal effects on Escherichia Coli," *Biomaterials*, vol. 31, no. 12, pp. 3317–3326, 2010.

[40] S. A. Elfeky and A.-S. A. Al-Sherbini, "Photo-oxidation of rhodamine-6-G via TiO_2 and Au/TiO_2 -bound polythene beads," *Journal of Nanomaterials*, vol. 2011, Article ID 570438, 8 pages, 2011.

[41] C. A. Castro, A. Jurado, D. Sissa, and S. A. Giraldo, "Performance of Ag-TiO_2 photocatalysts towards the photocatalytic disinfection of water under interior-lighting and solar-simulated light irradiations," *International Journal of Photoenergy*, vol. 2012, Article ID 261045, 10 pages, 2012.

[42] H. Zhu, B. Yang, J. Xu et al., "Construction of Z-scheme type CdS-Au-TiO_2 hollow nanorod arrays with enhanced photocatalytic activity," *Applied Catalysis B*, vol. 90, no. 3-4, pp. 463–469, 2009.

[43] N. Guijarro, T. Lana-Villarreal, I. Mora-Seró, J. Bisquert, and R. Gómez, "CdSe quantum dot-sensitized TiO2 electrodes: effect of quantum dot coverage and mode of attachment," *Journal of Physical Chemistry C*, vol. 113, no. 10, pp. 4208–4214, 2009.

[44] E. A. Rozhkova, I. Ulasov, B. Lai, N. M. Dimitrijevic, M. S. Lesniak, and T. Rajh, "A High-performance nanobio photocatalyst for targeted brain cancer therapy," *Nano Letters*, vol. 9, no. 9, pp. 3337–3342, 2009.

[45] W. H. Suh, K. S. Suslick, G. D. Stucky, and Y. H. Suh, "Nanotechnology, nanotoxicology, and neuroscience," *Progress in Neurobiology*, vol. 87, no. 3, pp. 133–170, 2009.

[46] J.-C. Sin, S.-M. Lam, A. R. Mohamed, and K.-T. Lee, "Degrading endocrine disrupting chemicals from wastewater by TiO_2 photocatalysis: a review," *International Journal of Photoenergy*, vol. 2012, Article ID 185159, 23 pages, 2012.